罗涛, 卿丽媛, 刘金雨, 等. 激光剥蚀电感耦合等离子体质谱法测定碳酸盐矿物中元素组成[J]. 岩矿测试, 2023, 42(5): 996−1006. doi: 10.15898/j.ykcs.202308020117.
LUO Tao, QING Liyuan, LIU Jinyu, et al. Accurate Determination of Elemental Contents in Carbonate Minerals with Laser Ablation Inductively Coupled Plasma-Mass Spectrometry[J]. Rock and Mineral Analysis, 2023, 42(5): 996−1006. doi: 10.15898/j.ykcs.202308020117.

激光剥蚀电感耦合等离子体质谱法测定碳酸盐矿物中元素组成

罗涛，卿丽媛，刘金雨，张文，何焘，胡兆初
(中国地质大学(武汉)地质过程与矿产资源国家重点实验室，湖北 武汉 430074)

摘要：碳酸盐中微量元素信息可为探究古环境、古气候演化、壳幔相互作用以及成岩成矿等重要地质作用过程提供关键约束，其微量元素含量的准确测定一直备受学者关注。激光剥蚀电感耦合等离子体质谱(LA-ICP-MS)可提供碳酸盐矿物中微量元素含量的精细信息，而常规激光测试方法严重制约着碳酸盐矿物微量元素分析的空间分辨率和低含量元素的检测能力。相比于常规剥蚀池条件时的低频率分析，本研究通过采用气溶胶局部提取快速清洗剥蚀池结合高频率激光剥蚀的方式，快速提升激光微区分析瞬时信号强度，有效地提升峰形信号灵敏度(约 13 倍)，碳酸盐激光微区元素检出限降低 5～10 倍。在此激光分析模式下，分别采用纳秒和飞秒激光剥蚀联用四极杆等离子体质谱仪(LA-Q-ICP-MS)，以 NIST610 玻璃为外标，Ca 为内标开展了较小激光剥蚀束斑(32μm)条件下碳酸盐矿物中微量元素(亲石元素、亲铁和亲硫元素)分析。结果表明，纳秒和飞秒激光分析碳酸盐矿物标样 CGSP-A、CGSP-B、CGSP-C、CGSP-D 和 MACS-3 获得的亲石元素(如 Sc、Sr、Y、Ba、La、Ce、Pr、Nd、Sm、Eu、Gd、Tb、Dy、Ho、Er、Tm、Yb 和 Th 等)测试值与推荐值在误差范围内一致；而亲铁和亲硫元素(如 Ni、Cu、Zn、As、Cd、Sn、Sb 和 Pb)测试结果则存在较大偏差(大于 20%)，这可能与本研究选用的高频激光剥蚀和较小剥蚀束斑(32μm)造成显著的“Downhole”分馏效应有关。本研究通过研制新型激光剥蚀池，改变激光剥蚀方式，即采用气溶胶局部提取剥蚀池和高频率剥蚀方法可有效地提升碳酸盐矿物微量元素(如亲石元素)分析的空间分辨率和低含量元素检测能力，有利于促进碳酸盐矿物在地质环境等领域的广泛应用。

关键词：激光剥蚀电感耦合等离子体质谱法；碳酸盐矿物；微量元素；气溶胶局部提取；高频率激光剥蚀

要点：

(1)采用气溶胶局部提取剥蚀方式相比于常规剥蚀池可使激光瞬时信号提高约 13 倍。

(2)高频率激光剥蚀相比于常规低频剥蚀可提高激光瞬时信号强度 1.5 倍。

(3)利用本研究提出的气溶胶局部提取剥蚀池结合高频率激光剥蚀方式可使碳酸盐矿物激光微区分析元素检出限降低 5～10 倍。

(4)实现 LA-Q-ICP-MS 较小剥蚀束斑(32μm)条件下准确测定碳酸盐矿物中的亲石元素含量。

中图分类号：P575；P578.6；O657.63 **文献标识码：**A

碳酸盐矿物广泛存在于火成岩、变质岩和沉积岩等各类岩石中，该类矿物元素含量组成为探究古环境、古气候演化、壳幔相互作用以及成岩成矿等重要地质作用过程提供关键信息[1-3]。因此，碳酸盐

收稿日期：2023−08−02；**修回日期：**2023−09−03；**接受日期：**2023−09−15
基金项目：国家重点研发计划项目 (2021YFC2903003) 课题“战略性矿产微区原位分析技术及应用”；国家自然科学基金项目 (41903015)；地质过程与矿产资源国家重点实验室专项
作者简介：罗涛，博士，副研究员，主要从事激光剥蚀等离子体质谱机理、元素及同位素分析和副矿物 U-Th-Pb 年代学研究。E-mail：luotao11@cug.edu.cn。

中微量元素含量的准确测定一直受到学者们的关注[4-7], 并在地质环境等领域取得广泛应用[8-10]。常用于碳酸盐中微量元素分析的方法有电感耦合等离子体发射光谱法(ICP-OES)[11]和等离子体质谱法(ICP-MS)[12-13]等整体分析技术, 以及激光剥蚀电感耦合等离子体质谱(LA-ICP-MS)等微区分析手段。整体分析技术(如溶液等离子体质谱法)测定碳酸盐矿物中的微量元素虽然具有非常高的准确度和低的检出限, 但其样品前处理流程复杂且无法提供原位信息, 这限制了对具有环带特征碳酸盐样品的精细分析[14-15]。LA-ICP-MS 技术具有仪器灵敏度高、空间分辨率高、样品量消耗少、样品前处理步骤简单等优点, 可开展各种样品中元素含量和同位素比值的快速准确分析[16-20]。

LA-ICP-MS 技术已被广泛应用于碳酸盐矿物中元素含量的测定[5, 21-22], Mertz-Kraus 等[21]采用外标结合内标法准确测定了碳酸盐的主微量元素, Chen 等[5]也采用总量归一化法准确测定了碳酸盐矿物中元素含量, 该方法避免了采用其他方法测定内标元素含量的繁琐步骤。不管采用何种校正方法, 标样与碳酸盐矿物基体间分析行为的差异是影响碳酸盐矿物元素含量准确测定的主要因素, 这种基体效应在开展高空间分辨率分析时尤为显著[5, 23]。Jochum 等[23]研究表明采用 NIST 玻璃为外标可准确测定碳酸盐中的亲石元素(如 Mg、Sr、Ba 和 U 等), 而亲硫或亲铁元素则需要基体匹配的碳酸盐标样校正才能获得准确的分析结果。Chen 等[5]研究结果表明, 在较小激光剥蚀束斑(32μm)时, 以玻璃为外标会观察到测试结果约 20% 或以上的偏差; 而在剥蚀束斑为 44μm 或更大时系统偏差则可以降低至 5% ~ 10%[5, 21, 24]。另一方面, 大部分碳酸盐中的稀土元素(REE)含量较低, 如石笋样品中含量通常为几百 pg/g 至几十 ng/g[25], 这对仪器灵敏度提出了更高要求。为克服常规四极杆等离子体质谱(Q-ICP-MS)对碳酸盐样品低含量元素检测灵敏度不足的限制[26], 大部分学者采用高灵敏度磁质谱进行碳酸盐矿物中微量元素的激光微区分析[6, 23, 26]。当前, LA-ICP-MS 开展碳酸盐矿物微量元素分析的主要问题为: ①对低含量元素检测能力有限, 为获得准确分析结果, 通常采用较大剥蚀束斑(44 ~ 100μm); ②激光分析空间分辨率有待进一步提高。

相比于纳秒激光剥蚀, 飞秒激光脉冲宽度短[27], 激光与样品相互作用时能量耦合更有效且热效应更小[28], 剥蚀产生的样品气溶胶颗粒更细小, 有利于气溶胶的传输和离子化, 因此飞秒激光剥蚀可有效地降低基体效应, 实现非基体匹配分析[29-30]。采用飞秒激光剥蚀在抑制玻璃标样和碳酸盐矿物基体效应方面具有巨大潜力。此外, 前人研究表明采用快速吹扫剥蚀池[31-34]和高频率激光剥蚀模式[19, 35]可以极大地提高 LA-ICP-MS 分析的信噪比, 降低仪器分析检出限。Hu 等[33]采用气溶胶局部提取策略获得的单脉冲信号清洗时间缩短约 12 倍, 且信号强度提升 13.5 倍。冯彦同等[35]通过高频激光剥蚀(20Hz)获得的最大信号强度是低频率激光剥蚀模式(5Hz)的 4.2 倍, 最终计算的元素分析检出限相比于低频率剥蚀降低了约 5 倍。以上两种有效提升激光微区分析信噪比的方法在提升碳酸盐样品微区分析空间分辨率和低含量元素检测能力方面具有广阔应用前景。

为提升碳酸盐矿物激光微区元素检测能力, 本文将通过研制激光剥蚀池和改进激光剥蚀方式等手段, 提高碳酸盐矿物 LA-ICP-MS 分析信噪比, 对比研究纳秒和飞秒激光剥蚀对碳酸盐矿物微量元素测定的影响。

1　实验部分

为进一步提升激光微区碳酸盐矿物微量元素分析的准确度、空间分辨率和低含量元素检测能力, 本文将采用气溶胶局部提取剥蚀池[36]结合高频率激光剥蚀方式, 以降低元素分析检出限, 提升碳酸盐矿物中低含量元素的检测能力。此外, 本文还将分别采用纳秒和飞秒激光剥蚀对比研究 NIST610 玻璃和碳酸盐矿物间微量元素分析的基体效应。

1.1　实验仪器

本实验在中国地质大学(武汉)地质过程与矿产资源国家重点实验室进行, 采用安捷伦公司的 7900 型四极杆质谱仪(Agilent Technology, Tokyo, Japan)分别与相干公司的 193nm 准分子纳秒激光(Geolas HD, MicroLas Göttingen, Germany)和 ESL 公司的 257nm Yb 飞秒激光剥蚀系统(NWR-Femto^{UC}, USA)联用。详细的实验参数列于表 1。

1.2　实验样品

本研究中仪器测试条件优化采用美国国家标准与技术研究所(NIST)合成的玻璃 NIST610[37], 通过调试气体流速及透镜参数使$^{139}La^+$信号到最大灵敏度, 同时氧化物产率 ThO^+/Th^+低于 0.3%, U^+/Th^+比值接近 1。当前用于碳酸盐矿物微量元素分析的标样均为人工合成, 主要有美国地质调查局(USGS)研制

表 1　LA-ICP-MS 仪器操作参数

Table 1　Summary of instrumental operating parameters.

激光剥蚀系统			Agilent 7900 电感耦合等离子体质谱仪	
工作参数	实验条件	实验条件	工作参数	实验条件
激光类型	193nm, 纳秒激光	257nm, 飞秒激光	RF 功率	1500W
剥蚀频率	6Hz, 20Hz	10Hz, 100Hz	等离子体气流速	15.0L/min
脉冲宽度	15ns	300fs	辅助气流速	1.0L/min
能量密度	6J/cm^2	2.5J/cm^2	采样深度	5.0mm
束斑大小 剥蚀模式	32μm 单点剥蚀	32μm 单点剥蚀	离子透镜设置	Typical
剥蚀时间	5s	5s	测量的同位素	^{43}Ca, ^{45}Sc, ^{51}V, ^{53}Cr, ^{55}Mn, ^{57}Fe, ^{59}Co, ^{60}Ni, ^{63}Cu, ^{66}Zn, ^{75}As, ^{88}Sr, ^{89}Y, ^{93}Nb, ^{111}Cd, ^{118}Sn, ^{121}Sb, ^{137}Ba, ^{139}La, ^{140}Ce, ^{141}Pr, ^{143}Nd, ^{147}Sm, ^{151}Eu, ^{157}Gd, ^{159}Tb, ^{163}Dy, ^{165}Ho, ^{166}Er, ^{169}Tm, ^{173}Yb, ^{175}Lu, ^{178}Hf, ^{181}Ta, ^{208}Pb, ^{232}Th, ^{238}U
			驻留时间	4ms
			检测器模式	Dual

的 MACS-1、MACS-3 和 GP-4, 以及中国地质调查局国家地质实验测试中心研制的 CGSP 系列。本研究选用实验室收集到的碳酸盐标准样品 MACS-3 和 CGSP 碳酸盐系列标样 CGSP-A、CGSP-B、CGSP-C 和 CGSP-D。

1.3　定量分析策略

为实现碳酸盐中低含量元素的激光微区分析, 本研究采用增加激光剥蚀频率的方式提高仪器灵敏度。在激光高频剥蚀条件下若进行常规剥蚀时间(约 40 ~ 50s)分析则会显著增加激光剥蚀时的“down-hole”分馏效应, 因此本研究选用高频激光剥蚀和短剥蚀时间(5s)开展碳酸盐微量元素分析。该剥蚀方法获得的原始数据信号与气相或液相色谱类似均为峰形信号(图 1a), 前人通常采用线性回归拟合对峰形瞬时数据进行处理[38-40], 本研究也采用线性回归拟合方法进行数据计算, 将待测元素(i)与内标元素(Ca)的原始信号进行线性拟合, 计算的拟合曲线斜率即为元素 i 与内标元素 Ca 的比值(图 1b), 线性回归拟合计算采用 Excel 函数进行。如图 1b 所示, 拟合曲线斜率 3.7385 即为 Ca/Mg 信号比值; 拟合度 R^2 为 0.9865, 展现出较好的线性拟合程度。最后, 碳酸盐微量元素定量分析以 NIST610 玻璃为外标, Ca 为内标进行校正。

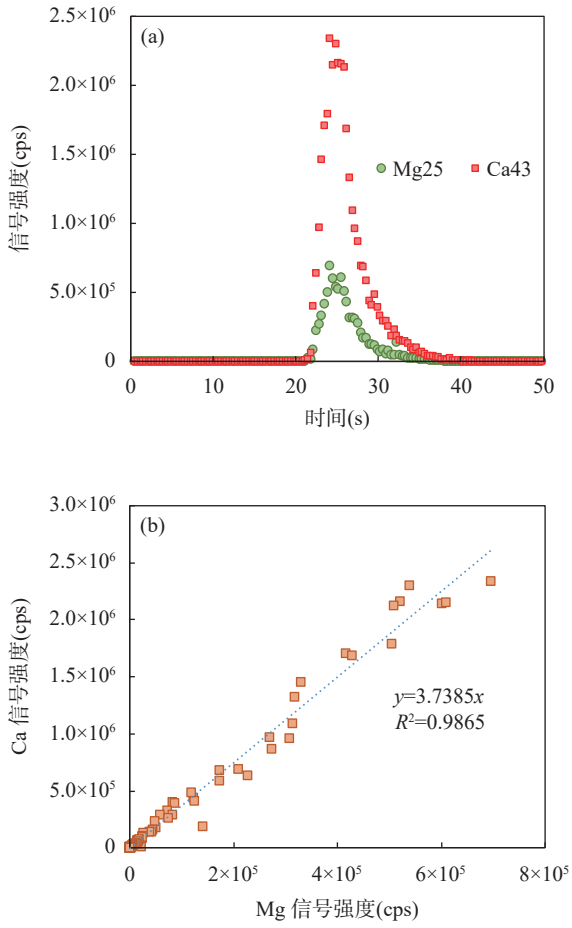

(a)飞秒激光高频率剥蚀碳酸盐标准样品 MACS-3 时 Mg，Ca 瞬时信号图；(b)线性回归拟合计算 Mg/Ca 比值。激光剥蚀束斑 32μm，剥蚀频率 50Hz。

(a) Magnesium and calcium signal of fs-LA on carbonate MACS-3; (b) The Mg/Ca ratio calculated with linear regression method. Laser ablation was performed with a spot size of 32μm and a repetition rate of 50Hz.

图1　定量分析示意图

Fig. 1　Schematic drawing of calibration.

2　结果与讨论

2.1　气溶胶局部提取剥蚀池

本研究采用气溶胶局部提取剥蚀池以进一步提升碳酸盐微量元素分析时峰形信号的灵敏度。气溶胶局部提取剥蚀池详细信息见文献 [33-34, 36, 41],

在 GeoLas HD 激光剥蚀系统标准剥蚀池的基础上改变其进出气口设置, 增加进气口直径, 减小出气口直径并将其引入剥蚀池内部, 该装置可在剥蚀点高速(可高达 10m/s)提取气溶胶颗粒, 降低样品清洗时间[36, 41]。分别在气溶胶局部提取和常规剥蚀池条件下采用纳秒激光单脉冲剥蚀 NIST610 玻璃时元素 U 瞬时信号如图 2 所示。在气溶胶局部提取模式时, 获得的信号强度比正常剥蚀高约 13 倍, 气溶胶清洗时间缩短约 12 倍(图 2)。在高频率激光剥蚀模式时获得的 U 元素峰形信号如图 3 所示, 纳秒激光剥蚀频率设定为最大值 20Hz, 剥蚀时间 5s, 此时采用气溶胶局部提取方式获得的最大信号强度是常规剥蚀池的 1.5 倍。因此, 采用气溶胶局部提取剥蚀池有利于提高高频剥蚀时峰形信号强度。本研究中碳酸盐微量元素测试选用气溶胶局部提取剥蚀池进行。

2.2　元素分析检出限

提高 LA-ICP-MS 分析灵敏度, 降低元素分析检出限是实现激光微区碳酸盐矿物低含量微量元素准确测定的关键。学者们通过向等离子体中引入氮气和水蒸气等活性气体可观察到显著的信号增敏[36, 42], 或者改变接口锥组合[43-44]和提高真空[45]也可显著增加质谱灵敏度, 从而降低元素分析检出限。本研究中不同激光条件下剥蚀碳酸盐元素检出限结果如图 4 所示。检出限计算参考 Longerich 等[46], 背景计算均选取剥蚀开始前 15s 气体背景, 峰形信号中选取最大值为信号强度, 则参

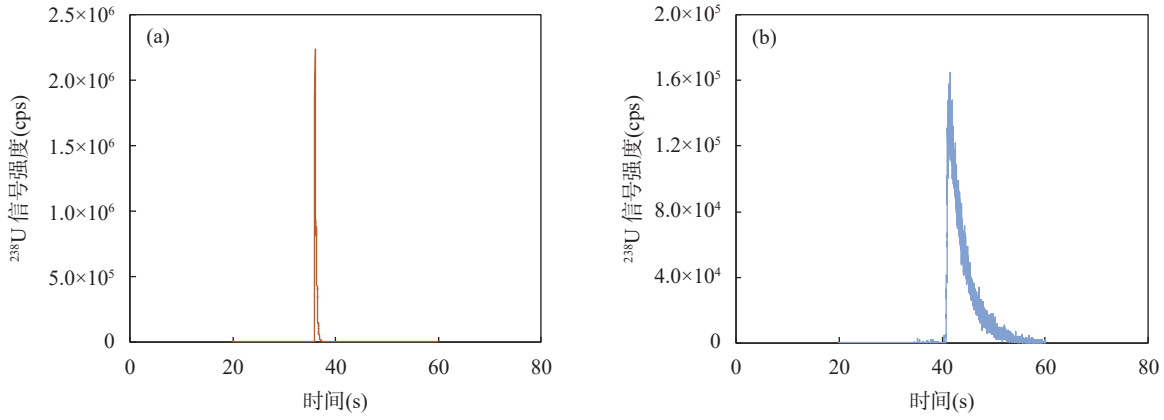

(a)气溶胶局部提取；(b)常规剥蚀池。激光剥蚀束斑 44μm。

(a) The local aerosol extraction ablation cell; (b) The normal ablation cell. Laser ablation was performed with a spot size of 44μm.

图2　气溶胶局部提取和常规剥蚀池纳秒激光单脉冲剥蚀 NIST610 玻璃时 U 元素瞬时信号对比图

Fig. 2　Uranium signal profile of single shot ablation on NIST610 glass with local aerosol extraction and normal ablation cell.

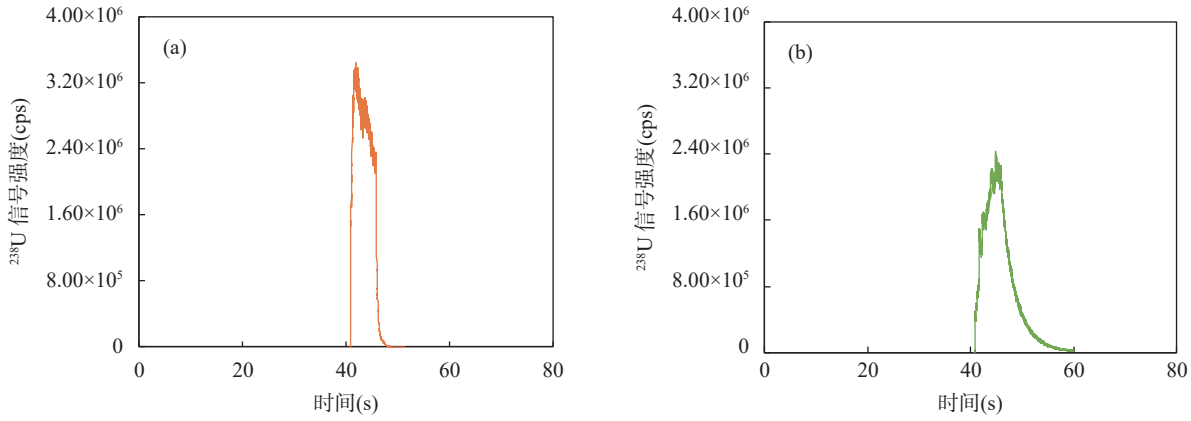

(a)气溶胶局部提取；(b)常规剥蚀池。激光剥蚀束斑 32μm，剥蚀频率 20Hz。

(a) The local aerosol extraction ablation cell; (b) The normal ablation cell. Laser ablation was performed with a spot size of 32μm and a repetition rate of 20Hz.

图3　纳秒激光高频率剥蚀 NIST610 玻璃时气溶胶局部提取和常规剥蚀池 U 元素瞬时信号对比图

Fig. 3　Uranium signal profile obtained with high repetition rates ns-laser ablation on NIST610 glass with local aerosol extraction and normal ablation cell.

与计算的剥蚀信号计数为 1，不同剥蚀条件下碳酸盐中常见微量元素的检出限见图 4。如图 4a 所示，在纳秒激光剥蚀时，剥蚀束斑 32μm、剥蚀频率 6Hz 的低频常规剥蚀条件下，获得的各元素检出限为 0.02 ~ 1.76μg/g；将剥蚀频率设置为最大值 20Hz，并结合气溶胶局部提取方式获得的元素检出限为 0.002 ~ 0.60μg/g，相比于常规分析，元素检出限降低约 5 ~ 8 倍。飞秒激光剥蚀束斑 32μm，剥蚀频率分别为 10Hz 和 100Hz 时获得的各元素检出限为 0.02 ~ 1.49μg/g 和 0.003 ~ 0.63μg/g（图 4b），元素检出限减低约 5 ~ 10 倍。以上研究结果表明，本文通过气溶胶局部提取方式结合高频率激光剥蚀可显著提高激光微区分析时瞬时信号强度，进而极大降低碳酸盐矿物激光微区分析的元素检出限。

2.3　碳酸盐标样微量元素分析结果

为准确测定碳酸盐中微量元素含量，本文以 NIST610[37] 玻璃为外标，Ca 为内标元素分析碳酸盐标准样品 MACS-3、CGSP-A、CGSP-B、CGSP-C 和 CGSP-D 中常见的微量元素。选用的激光和分析参数分别为：①纳秒激光结合气溶胶局部提取剥蚀池，剥蚀束斑 32μm、剥蚀频率 20Hz；②飞秒激光剥蚀束斑 32μm、剥蚀频率 100Hz。测试结果如图 5 和表 2 所示，纳秒激光剥蚀碳酸盐 MACS-3 和 CGSP 系列碳酸盐标样 CGSP-A、CGSP-B、CGSP-C 和 CGSP-D 时，获得的大部分亲石元素（Sc、Sr、Y、Ba、La、Ce、Pr、Nd、Sm、Eu、Gd、Tb、Dy、Ho、Er、Tm、Yb 和 Th 等）结果与推荐值偏差在 20% 内，测试值与推荐值在误差范围内一致。而元素 Lu、Hf 和 Ta 测试值偏差大于 20%，这可能与这些元素含量较低（约 0.3μg/g）或在激光剥蚀束斑 32μm 尺度内分布的均匀性较差有关。亲铁和亲硫元素（如 Ni、Cu、Zn、As、Cd、Sn、Sb 和 Pb）的测试结果偏差较大（大于 20%），

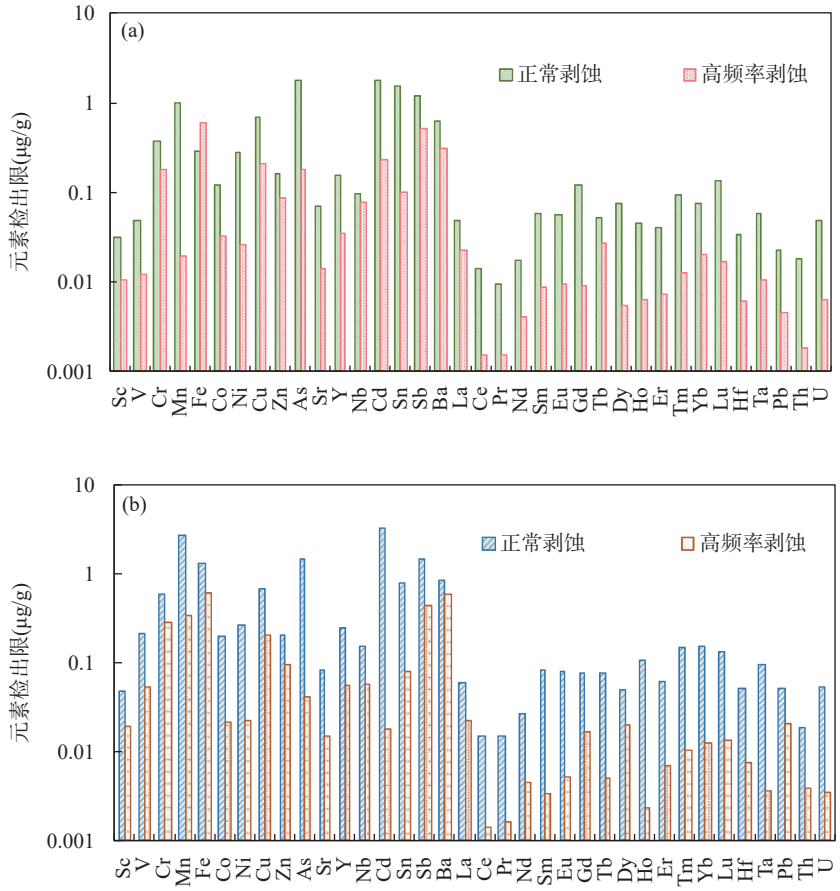

(a)纳秒激光常规剥蚀(剥蚀频率 6Hz)和气溶胶局部提取结合高频率剥蚀(20Hz)；
(b)飞秒激光常规剥蚀(剥蚀频率 10Hz)和高频率剥蚀(100Hz)。
(a) Nanosecond laser ablation with normal repetition rate (6Hz) and local aerosol extraction combined with high repetition rate (20Hz);
(b) Femtosecond laser ablation with normal repetition rate (10Hz) and high repetition rate (100Hz).

图4　不同激光剥蚀条件下元素检出限

Fig. 4　The limits of detection obtained under different laser ablation conditions.

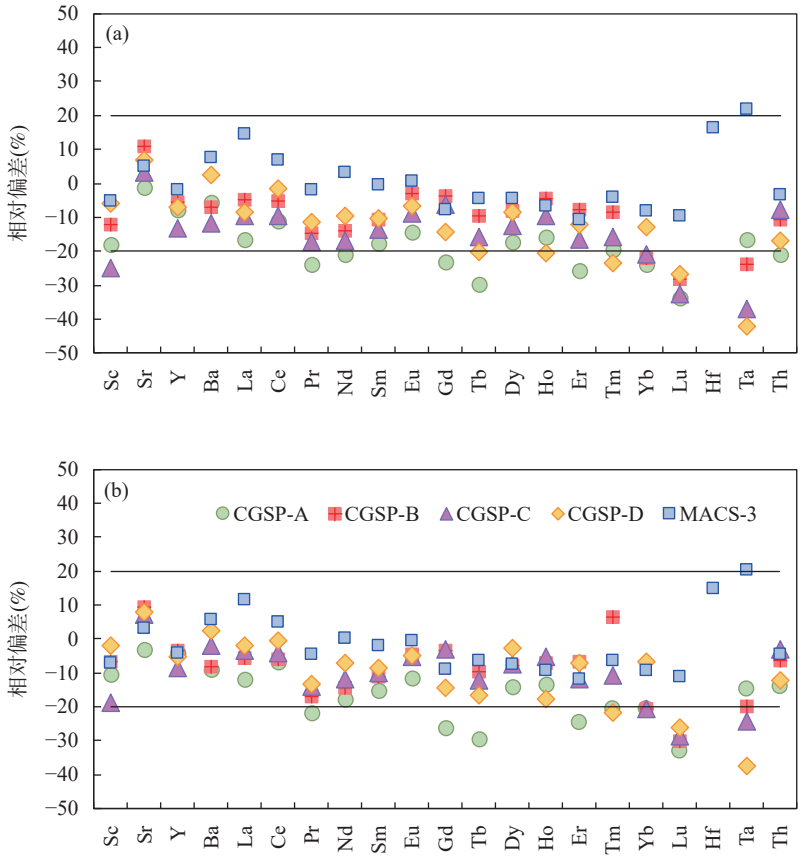

(a)纳秒激光气溶胶局部提取结合高频率剥蚀(20Hz)；(b)飞秒激光高频率剥蚀(100Hz)。剥蚀束斑均为 32μm。

(a) Nanosecond laser ablation with local aerosol extraction combined with high repetition rate (20Hz);

(b) Femtosecond laser ablation with high repetition rate (100Hz). The laser ablation spot size was 32μm.

图5　以 NIST610 玻璃为外标，Ca 为内标分析碳酸盐标样 CGSP-A、CGSP-B、CGSP-C、CGSP-D 和 MACS-3 结果

Fig. 5　The relative deviations of the measured average concentrations of carbonate reference materials (CGSP-A, CGSP-B, CGSP-C, CGSP-D and MACS-3). The NIST 610 glass was used as an external calibration material and Ca was used as an internal standard.

该结果与 Jochum 等[23]研究结果类似，说明在较小激光剥蚀束斑时(32μm)NIST610 玻璃和碳酸盐间存在显著基体效应，导致亲硫和亲铁元素测试结果的偏差。飞秒激光测试 CGSP 系列标样和碳酸盐 MACS-3 结果如图 5b 和表 2 所示，与纳秒激光结果类似，亲石元素的测试值与推荐值在误差范围内一致，而亲铁和亲硫元素则呈现出较大的系统偏差(20% 以上)。

以上研究结果表明选用 NIST610 玻璃为外标，Ca 为内标可以准确测定碳酸盐中亲石元素，而由于 NIST610 玻璃和碳酸盐间基体性质差异，即使采用飞秒激光也无法消除亲铁、亲硫元素测试的系统偏差。另一方面，即使本研究采用较短的激光剥蚀时间(5s)，但高频激光剥蚀方式和较小的激光剥蚀束斑(32μm)仍可能造成显著的“Downhole”分馏效应[18]，因而导致亲硫、亲铁元素测试结果呈现显著系统偏差。在接下来的研究中可通过优化数据算法进行“Downhole”分馏校正，实现较高空间分辨率条件下(32μm)碳酸盐矿物亲铁和亲硫元素的准确测定。相比于前人研究[5, 21-22]采用较大激光剥蚀束斑(44 ~ 100μm)开展碳酸盐矿物微量元素分析，本文实现了较小剥蚀束斑(32μm)时以 NIST 玻璃为外标实现碳酸盐亲石元素的准确分析。

3　结论

通过使用气溶胶局部提取剥蚀池结合激光高频剥蚀提高激光分析瞬时信号强度约 13 倍。采用此种激光剥蚀方式开展碳酸盐矿物微量元素分析，纳秒激光剥蚀高频率(20Hz)分析获得的元素检出限相比于常规分析(6Hz)降低约 5 ~ 8 倍；飞秒激光剥蚀频率从 10Hz 提升到 100Hz 时元素检出限降低约 5 ~ 10 倍。本研究实现了在较小激光剥蚀束斑条件

表 2　碳酸盐标样 LA-ICP-MS 分析结果（n=11）

Table 2　Element concentrations of carbonate reference materials obtained with LA-ICP-MS analysis (n=11).

元素	CGSP-A			CGSP-B			CGSP-C			CGSP-D			MACS-3		
	推荐值 (μg/g)	纳秒激光测定值 (μg/g)	飞秒激光测定值 (μg/g)	推荐值 (μg/g)	纳秒激光测定值 (μg/g)	飞秒激光测定值 (μg/g)	推荐值 (μg/g)	纳秒激光测定值 (μg/g)	飞秒激光测定值 (μg/g)	推荐值 (μg/g)	纳秒激光测定值 (μg/g)	飞秒激光测定值 (μg/g)	推荐值 (μg/g)	纳秒激光测定值 (μg/g)	飞秒激光测定值 (μg/g)
Sc	18.1±0.7	14.8±2.3	16.2±0.6	4.39±0.49	3.86±0.21	4.09±0.21	5.09±0.52	3.83±0.25	4.13±0.12	15.7±0.8	14.8±0.5	15.4±0.3	21.0±0.8	19.9±1.1	19.5±1.4
V	20.4±3.2	20.7±3.6	22.5±1.1	17.6±2.1	16.8±0.7	17.3±0.5	15.5±3.1	12.5±1.4	14.9±1.2	5.41±3.10	4.35±0.17	4.27±0.08	46.3±1.1	57.3±6.0	56.7±5.3
Cr	25.5±0.9	25.0±5.4	27.6±1.4	25±1	4.65±1.07	6.00±1.75	18.8±2.2	4.87±2.39	5.39±1.33	3.39±0.53	4.09±3.74	2.51±0.23	117±5	142±16	140±15
Mn	349±852	404±8721	390±1082	257±542	299±2639	287±837	267±232	294±515	306±945	189±232	213±1337	214±300	536±28	615±59	601±52
Fe	118±3378	818±13633	933±2872	219±3026	158±6282	172±4773	222±3448	137±13175	172±15173	792±1126	659±2973	644±551	112±300	124±1231	123±1146
Co	5.04±0.15	4.36±0.62	4.56±0.13	0.75±0.07	0.42±0.09	0.46±0.09	0.78±0.06	1.21±0.83	0.99±0.52	2.32±0.21	2.19±0.24	2.02±0.07	57.1±2.0	57.4±4.1	57.1±4.1
Ni	4.35±1.74	5.16±0.96	5.52±0.28	5.6±1.2	1.37±0.77	2.06±1.38	6.34±1.33	1.39±0.55	2.41±2.89	6.25±1.34	8.36±1.84	7.25±0.69	57.4±4.9	69±4	68.3±4.2
Cu	2.15±0.29	0.42±0.53	1.34±1.52	3.07±0.11	-1.186±3.266	0.62±0.16	2.26±0.19	0.76±1.20	1.15±0.22	1.37±0.28	0.79±2.93	0.30±0.09	120±5	141±15	137±14
Zn	517±20	473±65	520±32	36.9±2.2	29.9±6.6	36.7±2.1	92.1±3.0	77.3±8.1	86.4±5.3	17.2±2.7	16.8±5.2	16.7±1.1	111±6	170±19	165±18
As	3.68±0.41	10.0±2.0	10.4±1.3	5.44±0.49	8.33±0.65	7.42±0.46	3.42±0.34	6.42±0.79	6.42±0.55	3.39±0.35	3.34±0.63	3.39±0.34	44.2±1.4	61.1±7.1	59.8±7.1
Sr	255±74	251±148	247±110	261±111	289±88	285±76	293±89	302±83	313±85	246±72	263±141	265±38	676±350	711±192	697±368
Y	108±18	99.1±11.4	103±5	97.1±1.9	91.8±2.5	93.8±2.4	158±7	137±4	145±4	28.3±0.6	26.3±0.8	26.8±0.4	20.6±0.0	20.2±0.7	19.8±1.0
Nb	3.55±0.24	2.49±0.46	2.69±0.11	4.11±0.49	2.94±0.18	2.95±0.07	3.16±0.35	1.96±0.28	2.47±0.23	0.44±0.07	0.29±0.03	0.28±0.01	35.2±3.1	56.9±5.2	56.6±4.9
Cd	4.81±0.49	2.66±0.47	3.45±0.51	0.22±0.02	0.1±0.2	0.38±0.32	0.63±0.08	0.26±0.21	0.52±0.08	1.05±0.15	0.49±0.20	0.78±0.10	54.6±2.2	62.4±10.0	60.1±9.2
Sn	10.1±0.9	12.2±2.7	11.5±0.7	2.7±0.1	3.47±0.32	3.65±0.16	2.26±0.12	2.78±0.47	3.20±0.39	0.39±0.12	1.44±0.42	1.24±0.14	58.1±8.8	56.3±4.8	55.0±4.4
Sb	0.43±0.12	0.28±0.09	0.27±0.03	1.84±0.22	1.98±0.34	1.87±0.11	0.21±0.04	0.21±0.05	0.22±0.06	0.09±0.05	0.057±0.024	0.051±0.012	20.6±1.1	28.2±3.0	27.6±2.8
Ba	68.6±1.9	64.8±10.7	62.5±4.4	31.6±1.4	29.4±1.3	29.0±0.9	18.1±0.7	16±1	17.8±0.9	283±17	291±14	290±4	58.7±2.0	63.3±3.0	62.1±3.0
La	109±36	916±110	966±55	124±4	118±3	117±3	225±6	203±7	217±6	62.3±1.7	57±2	61.0±0.7	10.4±0.5	11.9±0.6	11.6±0.7
Ce	260±29	231±282	242±142	437±14	414±11	411±12	750±24	679±17	719±19	132±2	130±12	132±1	11.2±0.3	12±0	11.8±0.7
Pr	388±10	295±34	304±16	81.3±2.6	69.4±2.0	67.4±1.6	137±7	114±3	118±3	17.3±0.4	15.3±1.0	15.0±0.1	12.1±0.2	11.9±0.8	11.5±0.8
Nd	153±48	121±144	125±61	407±12	351±10	349±8	675±23	562±17	596±16	63.9±2.8	57.7±2.2	59.3±0.8	11.0±0.4	11.4±0.5	11.0±0.7
Sm	154±5	127±15	131±6	79.9±2.6	71.4±3.1	71.0±1.5	136±4	117±4	122±3	9.17±0.24	8.25±1.18	8.39±0.17	11.0±0.3	11±1	10.8±0.9
Eu	32.3±1.1	27.6±3.1	28.5±1.5	24.0±0.5	23.3±1.0	22.9±0.4	40.9±1.5	37.4±0.8	38.8±0.9	2.73±0.10	2.55±0.11	2.60±0.06	11.8±0.1	11.9±0.7	11.8±0.6
Gd	77.0±15.9	59.2±7.2	56.8±2.9	58.3±2.8	56.1±1.9	56.4±1.3	97.0±1.3	91.1±2.5	94.2±2.0	6.94±0.70	5.94±0.41	5.95±0.08	10.8±0.3	9.96±0.52	9.83±0.54
Tb	8.37±0.78	5.88±0.65	5.89±0.34	7.72±0.33	6.99±0.22	6.98±0.24	12.8±0.7	10.8±0.2	11.2±0.3	1.09±0.06	0.87±0.06	0.91±0.02	10.4±0.0	9.96±0.46	9.76±0.57
Dy	30.9±1.1	25.5±2.9	26.5±1.3	31.2±1.0	28.7±1.1	28.8±0.7	50.4±2.2	44.1±1.7	46.7±1.2	5.61±0.17	5.14±0.23	5.46±0.14	10.7±0.5	10.2±0.5	9.91±0.67
Ho	4.70±0.11	3.96±0.50	4.07±0.27	4.28±0.14	4.10±0.17	3.98±0.09	6.52±0.09	5.90±0.19	6.18±0.14	1.31±0.10	1.04±0.06	1.08±0.03	11.3±0.1	10.6±0.5	10.2±0.7
Er	10.0±1.6	7.41±0.96	7.58±0.39	7.24±0.25	6.69±0.27	6.76±0.58	11.7±0.7	9.80±0.40	10.3±0.3	2.78±0.04	2.44±0.20	2.58±0.05	11.2±0.2	10±1	9.90±0.56
Tm	0.89±0.02	0.72±0.10	0.71±0.04	0.70±0.03	0.64±0.03	0.74±0.36	0.98±0.03	0.83±0.04	0.88±0.03	0.41±0.05	0.31±0.05	0.32±0.01	11.1±0.1	10.7±0.6	10.4±0.7
Yb	4.22±0.10	3.20±0.43	3.37±0.24	3.07±0.16	2.39±0.21	2.44±0.09	4.47±0.25	3.54±0.33	3.55±0.13	1.67±0.05	1.46±0.17	1.56±0.07	11.6±0.1	10.7±0.5	10.5±0.6
Lu	0.51±0.06	0.34±0.03	0.34±0.02	0.40±0.04	0.29±0.02	0.28±0.02	0.49±0.01	0.33±0.02	0.35±0.03	0.24±0.03	0.18±0.02	0.18±0.01	11.1±0.1	10±0	9.88±0.54
Hf	0.21±0.02	0.032±0.028	0.027±0.009	0.19±0.02	0.024±0.017	0.031±0.040	0.23±0.05	0.0093±0.0038	0.012±0.004	0.1±0.0	0.0024±0.0048	0.0026±0.0021	4.73±0.21	5.51±0.56	5.44±0.46
Ta	0.33±0.03	0.28±0.05	0.28±0.02	0.75±0.02	0.57±0.04	0.60±0.02	0.4±0.0	0.25±0.08	0.30±0.03	0.18±0.02	0.10±0.02	0.11±0.01	20.5±5.3	25±3	24.7±2.4
Pb	163±31	218±345	193±90	312±6	435±21	373±10	224±5	267±26	277±26	119±5	157±3	146±3	56.5±1.8	74.6±6.4	73.3±7.2
Th	167±7	132±18	144±9	7.76±0.44	6.94±0.24	7.26±0.19	9.97±0.42	9.21±0.24	9.68±0.24	1.96±0.16	1.63±0.10	1.73±0.03	55.4±1.1	53.6±2.6	52.9±3.1
U	0.07±0.01	0.063±0.019	0.063±0.005	0.03±0.01	0.0043±0.0039	0.0046±0.0011	0.02±0.01	0.0037±0.0026	0.0049±0.0024	0.02±0.01	0.039±0.107	0.0038±0.0017	1.52±0.04	1.67±0.39	1.79±0.42

下(32μm), 以 NIST610 玻璃为外标, Ca 为内标校正, 分别采用纳秒和飞秒激光准确测定了碳酸盐标样 CGSP 系列和碳酸盐 MACS-3 中亲石元素(如 Sc、Sr、Y、Ba、La、Ce、Pr、Nd、Sm、Eu、Gd、Tb、Dy、Ho、Er、Tm、Yb 和 Th 等)含量。值得指出的是, 若将本研究提出的激光剥蚀方式与高灵敏度磁质谱联用, 则有望进一步提升碳酸盐元素分析空间分辨率和超低含量元素检测能力。

在较小剥蚀束斑条件下(32μm)获得的亲铁、亲硫元素(如 Ni、Cu、Zn、As、Cd、Sn、Sb 和 Pb)测试结果则存在显著系统偏差, 这可能与本研究采用的高频激光剥蚀方式造成的“Downhole”分馏效应有关。在今后研究中可优化校正算法, 开展“Downhole”分馏校正, 实现高空间分辨率条件下碳酸盐样品中亲铁、亲硫元素的准确测试。

致谢: 衷心感谢中国地质调查局国家地质实验测试中心范晨子研究员提供 CGSP 碳酸盐系列标样。

Accurate Determination of Elemental Contents in Carbonate Minerals with Laser Ablation Inductively Coupled Plasma-Mass Spectrometry

LUO Tao, *QING Liyuan*, *LIU Jinyu*, *ZHANG Wen*, *HE Tao*, *HU Zhaochu*

(State Key Laboratory of Geological Processes and Mineral Resources, China University of Geosciences (Wuhan), Wuhan 430074, China)

HIGHLIGHTS

(1) The obtained peak height of a single laser shot was enhanced by a factor of 13 with the local aerosol extraction ablation cell.

(2) The transient signal intensities were increased by 1.5 times under high-repetition rate laser ablation mode.

(3) The limits of detection of trace elements in carbonate minerals were reduced by 5-10 times with the local aerosol extraction ablation cell combined with high-repetition rate laser ablation mode.

(4) Accurate elemental content of lithophile elements in carbonate reference materials can be measured with both ns and fs LA-Q-ICP-MS with a spot size of 32μm.

ABSTRACT

BACKGROUND: Trace element information in carbonates provides key constraints for investigating ancient environments, paleoclimate evolution, shell-mantle interactions, diagenesis and mineralization processes. The accurate determination of trace element content in carbonate minerals have always been a primary focus. Laser ablation-inductively coupled plasma-mass spectrometry (LA-ICP-MS) can provide detailed information on trace element content in carbonate minerals. However, the elemental concentrations in carbonate minerals are usually extremely low (from hundreds of pg/g to tens of ng/g). A large spot size (from 44 to 100μm) is often used for trace element measurements in carbonate minerals. Therefore, the detection capability of low-content elements in carbonate minerals and the spatial resolution of LA determination still need to be improved.

OBJECTIVES: To develop a new analytical method for determination of low-content trace elements in carbonate minerals with LA-ICP-MS.

METHODS: A new local aerosol extraction ablation cell was proposed in this study. Laser ablation was performed

using high-repetition rates with the new designed ablation cell. The elemental contents in carbonate reference materials MACS-3, CGSP-A, CGSP-B, CGSP-C, and CGSP-D were determined with both ns and fs LA-Q-ICP-MS with a spot size of 32μm. Here, NIST 610 glass was used as an external calibration material and Ca was used as an internal standard.

RESULTS: The obtained peak height of a single laser shot was enhanced by a factor of 13 with the local aerosol extraction ablation cell because of the rapid washout time. The signal intensities were increased by 1.5 times under high-repetition rate laser ablation mode. Therefore, the detection limits of trace elements in carbonate minerals obtained from nanosecond laser ablation at high repetition rates (20Hz) were reduced by 5-8 times compared to conventional analysis (6Hz). The detection limits of trace elements were reduced by 5-10 times with the frequency of femtosecond laser ablation increased from 10Hz to 100Hz. The elemental contents in carbonate reference materials were measured with both ns and fs LA-Q-ICP-MS with a spot size of 32μm. The obtained results of lithophile elements (e.g., Sc, Sr, Y, Ba, La, Ce, Pr, Nd, Sm, Eu, Gd, Tb, Dy, Ho, Er, Tm, Yb, and Th) in carbonate CGSP series and carbonate MACS-3 showed good agreement with their reference values. However, the measured results of siderophile and chalcophile elements (e.g., Ni, Cu, Zn, As, Cd, Sn, Sb, and Pb) showed systematic bias (>20%), which may be related to the "downhole" fractionation effect caused by the high-repetition rate laser ablation used in this study.

CONCLUSIONS: The new designed local aerosol extraction ablation cell combined with high-repetition rate laser ablation mode significantly improved the spital resolution and determination ability of low-content elements in carbonate minerals. The obtained results of lithophile elements in carbonate CGSP series and carbonate MACS-3 showed good agreement with their reference values using ns- and fs-LA-Q-ICP-MS with a spot size of 32μm. It is worth noting that the spatial resolution and the detection capability of ultra-low-content elements in carbonate minerals could be further improved with the proposed LA method combined with high-sensitivity magnetic sector mass spectrometry.

KEY WORDS: LA-ICP-MS; carbonate minerals; trace elements; local aerosol extraction; high-repetition rate laser ablation

参考文献

[1] Hori M, Ishikawa T, Nagaishi K, et al. Rare earth elements in a stalagmite from Southwestern Japan: A potential proxy for chemical weathering[J]. Geochemical Journal, 2014, 48(1): 73−84.

[2] Chen W, Simonetti A. *In-situ* determination of major and trace elements in calcite and apatite, and U-Pb ages of apatite from the Oka carbonatite complex: Insights into a complex crystallization history[J]. Chemical Geology, 2013, 353: 151−172.

[3] Chen C F, Liu Y S, Foley S F, et al. Carbonated sediment recycling and its contribution to lithospheric refertilization under the Northern North China Craton[J]. Chemical Geology, 2017, 466: 641−653.

[4] Webb G E, Kamber B S. Rare earth elements in Holocene reefal microbialites: A new shallow seawater proxy[J]. Geochimica et Cosmochimica Acta, 2000, 64(9): 1557−1565.

[5] Chen L, Liu Y S, Hu Z C, et al. Accurate determinations of fifty-four major and trace elements in carbonate by LA-ICP-MS using normalization strategy of bulk components as 100%[J]. Chemical Geology, 2011, 284(3-4): 283−295.

[6] Sun D Y, Liu J, Fan C Z, et al. New CGSP carbonate matrix reference materials for LA-ICP-MS analysis[J]. Geostandards and Geoanalytical Research, 2023, 47(1): 7−22.

[7] Desmarchelier J M, Hellstrom J C, McCulloch M T. Rapid trace element analysis of speleothems by ELA-ICP-

MS[J]. Chemical Geology, 2006, 231(1-2): 102−117.

[8] Fairchild I J, Treble P C. Trace elements in speleothems as recorders of environmental change[J]. Quaternary Science Reviews, 2009, 28(5-6): 449−468.

[9] Treble P, Shelley J, Chappell J. Comparison of high resolution sub-annual records of trace elements in a modern (1911—1992) speleothem with instrumental climate data from Southwest Australia[J]. Earth and Planetary Science Letters, 2003, 216(1-2): 141−153.

[10] Smrzka D, Zwicker J, Bach W, et al. The behavior of trace elements in seawater, sedimentary pore water, and their incorporation into carbonate minerals: A review[J]. Facies, 2019, 65: 1−47.

[11] Kawabe I, Kitahara Y, Naito K. Non-chondritic yttrium/holmium ratio and lanthanide tetrad effect observed in pre-Cenozoic limestones[J]. Geochemical Journal, 1991, 25(1): 31-44.

[12] 陈琳莹, 李崇瑛, 陈多福. 碳酸盐岩中碳酸盐矿物稀土元素分析方法进展[J]. 矿物岩石地球化学通报, 2012, 31(2): 177−183.
Chen L Y, Li C Y, Chen D F. Progress of analytical methods of rare earth elements of carbonate minerals in carbonate rocks[J]. Bulletin of Mineralogy, Petrology and Geochemistry, 2012, 31(2): 177−183.

[13] Akagi T, Hashimoto Y, Fu F, et al. Variation of the distribution coefficients of rare earth elements in modern coral-lattices: Species and site dependencies[J]. Geochimica et Cosmochimica Acta, 2004, 68(10): 2265−2273.

[14] Tan L, Shen C C, Cai Y, et al. Trace-element variations in an annually layered stalagmite as recorders of climatic changes and anthropogenic pollution in Central China[J]. Quaternary Research, 2014, 81(2): 181−188.

[15] Arkhipkin A I, Schuchert P C, Danyushevsky L. Otolith chemistry reveals fine population structure and close affinity to the Pacific and Atlantic oceanic spawning grounds in the migratory southern blue whiting (Micromesistius Australis)[J]. Fisheries Research, 2009, 96(2-3): 188−194.

[16] Jenner F E, Arevalo R D. Major and trace element analysis of natural and experimental igneous systems using LA-ICP-MS[J]. Elements, 2016, 12(5): 311−316.

[17] 刘勇胜, 胡兆初, 李明, 等. LA-ICP-MS 在地质样品元素分析中的应用[J]. 科学通报, 2013, 58(36): 3753−3769.
Liu Y S, Hu Z C, Li M, et al. Applications of LA-ICP-MS in the elemental analyses of geological samples[J]. Chinese Science Bulletin, 2013, 58(36): 3753−3769.

[18] 罗涛, 胡兆初. 激光剥蚀电感耦合等离子体质谱副矿物 U-Th-Pb 定年新进展[J]. 地球科学, 2022, 47(11): 4122−4144.
Luo T, Hu Z C. Recent advances in U-Th-Pb dating of accessory minerals by laser ablation inductively coupled plasma mass spectrometry Earth Science[J]. Earth Science, 2022, 47(11): 4122−4144.

[19] Liao X H, Hu Z C, Luo T, et al. Determination of major and trace elements in geological samples by laser ablation solution sampling-inductively coupled plasma mass spectrometry[J]. Journal of Analytical Atomic Spectrometry, 2019, 34(6): 1126−1134.

[20] Luo T, Wang Y, Li M, et al. Determination of major and trace elements in alloy steels by nanosecond and femtosecond laser ablation ICP-MS with non-matrix-matched calibration[J]. Atomic Spectroscopy, 2020, 41(1): 11−19.

[21] Mertz-Kraus R, Brachert T, Jochum K, et al. LA-ICP-MS analyses on coral growth increments reveal heavy winter rain in the Eastern Mediterranean at 9Ma[J]. Palaeogeography, Palaeoclimatology, Palaeoecology, 2009, 273(1-2): 25−40.

[22] Thompson J A, Thompson J M, Goemann K, et al. Use of non-matrix matched reference materials for the accurate analysis of calcium carbonate by LA-ICP-MS[J]. Geostandards and Geoanalytical Research, 2022, 46(1): 97−115.

[23] Jochum K P, Scholz D, Stoll B, et al. Accurate trace element analysis of speleothems and biogenic calcium carbonates by LA-ICP-MS[J]. Chemical Geology, 2012, 318: 31−44.

[24] Strnad L, Ettler V, Mihaljevic M, et al. Determination of trace elements in calcite using solution and laser ablation ICP - MS: Calibration to NIST SRM glass and USGS MACS carbonate, and application to real landfill calcite[J]. Geostandards and Geoanalytical Research, 2009, 33(3): 347−355.

[25] Bourdin C, Douville E, Genty D. Alkaline-earth metal and rare-earth element incorporation control by ionic radius and growth rate on a stalagmite from the Chauvet Cave, Southeastern France[J]. Chemical Geology, 2011, 290(1-2): 1−11.

[26] Wu C C, Burger M, Günther D, et al. Highly-sensitive open-cell LA-ICPMS approaches for the quantification of rare earth elements in natural carbonates at parts-per-billion levels[J]. Analytica Chimica Acta, 2018, 1018: 54−61.

[27] Russo R E, Mao X, Gonzalez J J, et al. Femtosecond laser ablation ICP-MS[J]. Journal of Analytical Atomic Spectrometry, 2002, 17(9): 1072−1075.

[28] Fernández B, Claverie F, Pécheyran C, et al. Direct analysis of solid samples by fs-LA-ICP-MS[J]. TrAC Trends in Analytical Chemistry, 2007, 26(10): 951−966.

[29] Bian Q, Garcia C C, Koch J, et al. Non-matrix matched calibration of major and minor concentrations of Zn and Cu in brass, aluminium and silicate glass using NIR femtosecond laser ablation inductively coupled plasma mass spectrometry[J]. Journal of Analytical Atomic Spectrometry, 2006, 21(2): 187−191.

[30] Horn I, von Blanckenburg F. Investigation on elemental and isotopic fractionation during 196nm femtosecond laser ablation multiple collector inductively coupled plasma mass spectrometry[J]. Spectrochimica Acta Part B:Atomic Spectroscopy, 2007, 62(4): 410−422.

[31] Neff C, Becker P, Günther D. Parallel flow ablation cell for short signal duration in LA-ICP-TOFMS element imaging[J]. Journal of Analytical Atomic Spectrometry, 2022, 37(3): 677−683.

[32] ,Becker P, Günther D. Reducing sample amount for forensic glass analysis using LA-ICP-TOFMS and multivariate statistics[J]. Journal of Analytical Atomic Spectrometry, 2023, 38: 1704-1712.

[33] Hu Z C, Liu Y S, Gao S, et al. A local aerosol extraction strategy for the determination of the aerosol composition in laser ablation inductively coupled plasma mass spectrometry[J]. Journal of Analytical Atomic Spectrometry, 2008, 23(9): 1192−1203.

[34] Luo T, Wang Y, Hu Z C, et al. Further investigation into ICP-induced elemental fractionation in LA-ICP-MS using a local aerosol extraction strategy[J]. Journal of Analytical Atomic Spectrometry, 2015, 30(4): 941−949.

[35] 冯彦同, 张文, 胡兆初, 等. 激光剥蚀电感耦合等离子体质谱仪新分析模式及其在地球科学中的应用[J]. 中国科学: 地球科学, 2022, 52(1): 98-121.
Feng Y T, Zhang W, Hu Z C, et al. A new analytical mode and application of the laser ablation inductively coupled plasma mass spectrometer in the Earth sciences[J]. Science China Earth Sciences, 2022, 65(1): 182−196.

[36] Luo T, Hu Z C, Zhang W, et al. Reassessment of the influence of carrier gases He and Ar on signal intensities in 193nm excimer LA-ICP-MS analysis[J]. Journal of Analytical Atomic Spectrometry, 2018, 33(10): 1655−1663.

[37] Jochum K P, Weis U, Stoll B, et al. Determination of reference values for NIST SRM 610-617 glasses following ISO guidelines[J]. Geostandards and Geoanalytical Research, 2011, 35(4): 397−429.

[38] Fietzke J, Liebetrau V, Günther D, et al. An alternative data acquisition and evaluation strategy for improved isotope ratio precision using LA-MC-ICP-MS applied to stable and radiogenic strontium isotopes in carbonates[J]. Journal of Analytical Atomic Spectrometry, 2008, 23(7): 955−961.

[39] Pettke T, Oberli F, Audétat A, et al. Quantification of transient signals in multiple collector inductively coupled plasma mass spectrometry: Accurate lead isotope ratio determination by laser ablation of individual fluid inclusions[J]. Journal of Analytical Atomic Spectrometry, 2011, 26(3): 475−492.

[40] Kappel S, Boulyga S, Dorta L, et al. Evaluation strategies for isotope ratio measurements of single particles by LA-MC-ICPMS[J]. Analytical and Bioanalytical Chemistry, 2013, 405: 2943−2955.

[41] 罗涛. LA-ICP-MS 分析过程中 ICP 引起的元素分馏效应研究[D]. 武汉: 中国地质大学 (武汉), 2015.
Luo T. Further investigation into ICP-induced elemental fractionation in LA-ICP-MS using a local aerosol extraction strategy[D]. Wuhan: China University of Geosciences (Wuhan), 2015.

[42] Hu Z C, Gao S, Liu Y S, et al. Signal enhancement in laser ablation ICP-MS by addition of nitrogen in the central channel gas[J]. Journal of Analytical Atomic Spectrometry, 2008, 23(8): 1093−1101.

[43] Hu Z C, Liu Y S, Gao S, et al. Improved *in situ* Hf isotope ratio analysis of zircon using newly designed X skimmer cone and jet sample cone in combination with the addition of nitrogen by laser ablation multiple collector ICP-MS[J]. Journal of Analytical Atomic Spectrometry, 2012, 27(9): 1391−1399.

[44] Wu S T, Yang M, Yang Y H, et al. Improved *in situ* zircon U-Pb dating at high spatial resolution (5-16μm) by laser ablation-single collector-sector field-ICP-MS using Jet sample and X skimmer cones[J]. International Journal of Mass Spectrometry, 2020, 456: 116394.

[45] Yuan H L, Bao Z A, Chen K Y, et al. Improving the sensitivity of a multi-collector inductively coupled plasma mass spectrometer *via* expansion-chamber pressure reduction[J]. Journal of Analytical Atomic Spectrometry, 2019, 34(5): 1011−1017.

[46] Longerich H P, Jackson S E, Günther D. Inter-laboratory note. Laser ablation inductively coupled plasma mass spectrometric transient signal data acquisition and analyte concentration calculation[J]. Journal of Analytical Atomic Spectrometry, 1996, 11(9): 899−904.